# Molecular Gradients of ω-Substituted Alkanethiols on Gold: Preparation and Characterization

Bo Liedberg* and Pentti Tengvall

*Laboratory of Applied Physics, Linköping University, S-581 83 Linköping, Sweden*

*Received April 3, 1995. In Final Form: June 6, 1995*[⊗]

A general methodology capable of generating a molecular, chemical concentration gradient on a solid substrate in one surface dimension is presented. Although the method can be extended to more than one surface dimension, and to a variety of molecule/substrate systems, we have chosen to demonstrate it by utilizing thiols on gold as the model system. The gradients are prepared by cross-diffusing ω-substituted alkanethiols, $HS(CH_2)_nX$ (X = OH, $CO_2CH_3$, COOH, and $CD_3$, $n = 10-19$), with or without fully deuterated chains, and simple *n*-alkanethiols, $HS(CH_2)_mY$ (Y = $CH_3$, $m = 9-17$), toward each other from opposite ends of a polysaccharide matrix deposited on top of a gold substrate. The so-prepared gradients are characterized by a number of techniques, including ellipsometry, contact angle measurements, and infrared reflection absorption spectroscopy (IRAS). The observed ellipsometric thicknesses and the limiting contact angles of the gradient assemblies agree very well with the values obtained from the corresponding single component and mixed self-assembled monolayers. The infrared data furthermore suggest that the entire gradient is composed of well-organized and densely packed *all-trans* hydrocarbon chains for thiols with chain length >10. The lateral dimensions of the gradient regions vary between 4 and 8 mm for the combination diffusion pairs employed in this study. The upper and lower values account for diffusion pairs with long and short hydrocarbon chains, respectively. It must be stressed, however, that the infrared and ellipsometric techniques only can provide information about the molecular organization on the macroscopic scale because of the relatively large spot size (≈1 mm) used in the experiments. Scanning probe microscopy must be employed to further investigate the mechanism of gradient formation, the molecular concentration profile, and mixing behavior on the microscopic (molecular) scale. We believe, however, that the large number of chemical and structural combinations attainable with the present approach can be used to address a broad range of surface physics/chemistry problems in material science and generate novel and unique model organic architectures. We discuss briefly the potential applications of these novel gradients in areas of relevance to molecular recognition and biosensing.

## Introduction

Self-assembly of organosulphur compounds on gold has developed into a widespread synthetic methodology for the preparation of structurally and chemically well-defined surface phases.[1-5] For example, the assembly of single-component and mixed monolayers of ω-substituted alkanethiols, $HS(CH_2)_nX$, offer an excellent opportunity to generate organic surface phases with molecular level control of alkyl chain conformation and orientation, composition, tail group functionality, and mobility. These surface phases, and those formed by spontaneous assembly of symmetrical and unsymmetrical sulfides and disulfides, are in many cases considered to be far more attractive and reliable than the corresponding Langmuir–Blodgett films, because of their improved stability and ease of preparation. As a consequence, they have been frequently utilized in diverse applications and contributed to a deeper theoretical and experimental understanding of phenomena like interfacial condensation and nucleation[6-9] and wetting.[3,10-12] They also have been used for immobilization of electroactive groups,[13-15] and molecular recognition sites,[16-20] as well as for more complex functions in biocompatibility[21,22] and biosensing[23] applications. Many developments today are directed toward molecular recognition processes on different levels of complexity. For example, gold–alkanethiol chemistry and advanced photolitographic techniques have been successfully combined to generate microstructured arrays with predefined size, shape, and chemistry[24-26] for protein adsorption and cell

⊗ Abstract published in *Advance ACS Abstracts,* August 15, 1995.

(1) Nuzzo, R. G.; Fusco, F. A.; Allara, D. L. *J. Am. Chem. Soc.* **1987**, *109*, 2358.
(2) Thoughton, E. B.; Bain, C. D.; Whitesides, G. M.; Nuzzo, R. G., Allara, D. L.; Porter, M. D. *Langmuir* **1988**, *4*, 365.
(3) Bain, C. D.; Thoughton, E. B.; Tao, Yu-Tai; Evall, J.; Whitesides, G.; Nuzzo R. G. *J. Am. Chem. Soc.* **1989**, *111*, 321.
(4) Nuzzo, R. G.; Dubois, L. H.; Allara, D. L., *J. Am. Chem. Soc.* **1990**, *112*, 558.
(5) Laibinis, P. E.; Whitesides, G. M.; Allara, D. L.; Tao, Yu-Tai, Parikh, A. N.; Nuzzo, R. G. *J. Am. Chem. Soc.* **1991**, *113*, 7152.
(6) Hautmann, J.; Klein, M. L. *Phys. Rev. Lett.* **1991**, *67*, 1763.
(7) Dubois, L. H.; Zegarski, B. R.; Nuzzo, R. G. *J. Am. Chem. Soc.* **1990**, *112*, 570.
(8) Nuzzo, R. G.; Zegarski, B. R.; Korenic, E. M.; Dubois, L. H. *J. Phys. Chem.* **1992**, *96*, 1355.
(9) Engquist, I.; Lundström, I.; Liedberg, B. *J. Phys. Chem.* In press.
(10) Bain, C. D.; Whitesides, G. M., *J. Am. Chem. Soc.* **1989**, *111*, 7164.
(11) Evans, S. D.; Sharma, R,; Ullman, A. *Langmuir* **1991**, *7*, 156.
(12) Folkers, J. P.; Laibinis, P. E.; Whitesides, G. M. *Langmuir* **1992**, *8*, 1330.
(13) Chidsey, C. E. D. *Science* **1991**, *251*, 919.
(14) Chidsey, C. E. D.; Bertozzi, C. R.; Putvinski, T. M.; Mujsce, A. M. *J. Amer. Chem. Soc.* **1990**, *112*, 4301.
(15) Finklea, H. O.; Hanshew, D. D. *J. Am. Chem. Soc.* **1992**, *114*, 3173.
(16) Schierbaum, K. D.; Weiss, T.; Thoden van Velzen, E. U.; Engbersen, J. F. J.; Reinhoudt, D. N.; Göpel, W. *Science* **1994**, *265*, 1413.
(17) Spinke, J.; Liley, M.; Guder, H.-J.; Angermaier, L.; Knoll, W. *Langmuir* **1993**, *9*, 1821.
(18) Häussling, L.; Ringsdorf, H.; Schmitt, F.-J.; Knoll, W. *Langmuir* **1991**, *7*, 1837.
(19) Spinke, J.; Liley, M.; Schmitt, F.-J.; Guder, H.-J.; Angermaier, L.; Knoll, W. *J. Chem. Phys.* **1993**, *99*, 7012.
(20) Häussling, L.; Michel, B.; Ringsdorf, H.; Rohrer, H. *Angew. Chem. Int. Ed. Engl.* **1991**, *30*, 569.
(21) Prime, K. L.; Whitesides, G. M. *Science*, **1991**, *252*, 1164.
(22) Pale-Grosdemange, C.; Simon, E. S.; Prime, K. L.; Whitesides, G. M. *J. Am. Chem. Soc.* **1991**, *113*, 12.
(23) Löfås, S.; Johnsson; B. *J. Chem. Soc. Chem. Commun.* **1990**, 1526.
(24) Singhvi, R.; Kumar, A.; Lopez, G. P.; Stephanopoulos, G. N.; Wang, D. I. C.; Whitesides, G. M.; Ingber; D. E. *Science* **1994**, *264*, 696.
(25) Lopez, G. P.; Biebuyck, H. A.; Whitesides, G. M. *Langmuir* **1993**, *9*, 1513.
(26) Lopez, G. P.; Albers, M. W.; Schreiber, R. C.; Peralta, E.; Whitesides, G. M. *J. Am. Chem. Soc.* **1993**, *115*, 5877.

0743-7463/95/2411-3821$09.00/0 

attachment studies. The technological impetus for such devices (arrays) rely primarily on the ability to create structures which ideally should have infinitesimally sharp boundaries, with a minimum of intermixing, between the adjacent surface phases.

The approach presented here is completely different and focuses on the development of a gradually changing interfacial region, "*a concentration gradient*", between two adjacent surface phases. This is the first report in a series describing a cross-diffusion methodology[27] enabling two alkanethiols $HS(CH_2)_nX/HS(CH_2)_mY$ to diffuse and intermix in a polysaccharide matrix and simultaneously bind to gold during formation of two opposing concentration gradients.

Molecular and chemical gradients have previously been prepared on $Si/SiO_2$ wafers[28-39] and on polymer surfaces.[40-42] Two different strategies have been employed to generate gradients on $Si/SiO_2$ wafers, and both are based on molecular diffusion in either the liquid[28,29] or the gas phase.[39] The molecular part of the so-prepared gradients consists of covalently attached alkylchlorosilane molecules and the other (nonmolecular) part of silanol groups on the $Si/SiO_2$ substrate itself. The vast majority of these gradients have been used for studies of protein adsorption,[31,38] and protein−protein[29,30,37] and protein−detergent[28,32-35] interaction phenomena. The gradients on polymeric substrates were prepared with either a scanning radio frequency (RF) discharge[40] or a scanning corona RF discharge[41,42] apparatus. By controlling the atmosphere, exposure time, and power of the discharge apparatuses, the investigators were able to vary the degree of oxidation of the outermost surface region of the polymer and thereby generating a chemical gradient along the substrate. For all of the above mentioned strategies of preparation, the substrate surface itself acts as one chemical (hydrophobic/hydrophilic) component in the gradient. Another common feature is that almost all of the gradients are referred to as *wettability gradients*, a limitation which, for the $Si/SiO_2$−alkylchlorosilane system, is related to the difficulties associated with the synthesis and handling of $\omega$-substituted alkylchlorosilanes. Very recently, however, Lin et al.[43] presented a novel gradient of isocyanopropyldimethylsilyl groups on silica. The idea was to hydrolyze the isocyanato group into an amine and to use the so-prepared amino gradient as a template for end point attachment of aldehyde-terminated poly(ethylene glycol), PEG. X-ray photoelectron spectroscopy, ellipsometry, and contact angle measurements revealed the existence of a PEG gradient region, approximately 7 mm long. The gradients were later utilized to study the adsorption characteristics of plasma protein mixtures.

The present approach is more general than the above mentioned methods and, most importantly, it does not rely on using the substrate surface as a component in the gradient. The richness of the synthetic protocols and compounds (thiols) available, with different chain lengths and/or tail groups, dramatically increases the flexibility and the number of possible chemical combinations in the gradient. Thus, one can easily envision gradients displaying a continuous change in wettability, charge, polarity, L- to D-isomerism, receptor site density, alkyl chain conformation, tail group mobility, etc. The latter two, for example, can be prepared by cross-diffusing thiols with different chain lengths. Here we report contact angle, ellipsometric, and infrared measurements of a series of $\omega$-substituted alkanethiols with fairly simple tail groups in order to establish the composition, alkyl chain conformation, and lateral dimensions of the gradients. The generality and applicability of these novel gradients for studies of laterally resolved surface phenomena of relevance, e.g., for biomolecular recognition and biosensing, are also discussed.

## Experimental Section

**Preparation of Gold Substrates.** Gold substrates were prepared by sputter deposition of chromium (~10 Å) followed by gold (~2000 Å) onto precut 40 × 4 × 0.3 (ellipsometry) and 20 × 20 × 0.3 mm (contact angles and IR) glass strips. The gold substrates were stored in closed containers until use. Prior to the gradient preparation, the gold substrates were cleaned in ethanol (95%).

**Chemicals.** The diffusion pairs chosen were selected from a series of long chain $\omega$-substituted alkanethiols, $HS(CH_2)_nX$, X = OH, COOH, $COOCH_3$ (gift from Pharmacia Biosensor AB, Uppsala, Sweden). Simple $n$-alkanethiols, $HS(CH_2)_mCH_3$ were obtained from Fluka. The deuterated analogs $HS(CD_2)_{19}CD_3$ and $HS(CD_2)_{10}COOH$ were obtained from Prof. D. L. Allara, The Pennsylvania State University. The thiols were dissolved in 95% ethanol (Kemetyl, Stockholm, Sweden) to a concentration of 2 mM. The diffusion medium consisted of hydroxypropylated and cross-linked dextran, Sephadex LH-20 (Pharmacia, Uppsala, Sweden), a matrix material that can be handled in water and organic solvents. All solvents used for cleaning or rinsing in this study were of analytical grade.

**Ellipsometry.** Ellipsometric measurements were performed with an automatic Rudolph Research AutoEl III ellipsometer aligned at an angle of incidence of 70° with respect to the surface normal. The ellipsometer was equipped with a He−Ne laser ($\lambda$ = 632.8 nm) light source and a scanning table (step size of 0.635 mm). The thicknesses of the gradient monolayers were calculated from the ellipsometric readings, $\Delta$ and $\Psi$, using a three-layer (parallel slab) model, Au/thiol/air, with isotropic optical constants for the organic layer, $N_{org} = n + ik = 1.50 + i0$, where $n$ is the refractive index and $k$ the extinction coefficient. Evaluating ellipsometric data obtained from a clearly anisotropic molecular film, with an isotropic model, may of course result in erroneous absolute thicknesses. On the other hand, the vast majority of the published ellipsometric data of single component and mixed monolayers of thiols on gold are based on an isotropic approach. We have therefore chosen to fit our ellipsometric data to an isotropic model since the the absolute thicknesses of the assemblies are of less importance for the determination of the gradient profiles. The optical constants for Au were calculated from the $\Delta$ and $\Psi$ values obtained from a clean, noncoated gold surface. The optical constants of Au were later used as input values for the calculation of the gradient thicknesses.

**Contact Angle Measurements.** The static contact angles with MilliQ water at the very extreme ends of the gradients were measured in laboratory atmosphere with the syringe method. The contact angle apparatus was equipped with a video camera system developed at our laboratory. At least three droplets were

(27) Patent pending.
(28) Elwing, H.; Welin, S.; Askendal, A.,; Nilsson, U.; Lundström, I. *J. Colloid Interface Sci.* **1987**, *119*, 203.
(29) Elwing, A.; Askendal, A.; Lundström, *I. Progr. Colloid Polym. Sci.* **1987**, *74*, 103.
(30) Elwing, H.; Askendal, A.; Lundström, I. *J. Biomed. Mater. Res.* **1987**, *21*, 1023.
(31) Elwing, H.; Welin, S.; Askendal, A.; Lundström, I. *J. Colloid Interface Sci.* **1988**, *123*, 306.
(32) Elwing, H.; Askendal, A.; Lundström, I. *J. Colloid Interface Sci.* **1989**, *128*, 296.
(33) Elwing, H.; Gölander, C.-G. *Adv. Colloid Interface Sci.* **1990**, *32*, 317.
(34) Welin-Klintström, S.; Askendal, A.; Elwing, H. *J. Colloid Interface Sci.* **1993**, *158*, 188.
(35) Wahlgren, M.; Welin-Klintström, S.; Arnebrant, T.; Askendal, A.; Elwing, H. *Colloids Surf. B: Biointerfaces* **1995**, *4*, 23.
(36) Hlady, V.; Gölander, C.-G.; Andrade, J. D. *Colloids Surf.* **1987**, *25*, 185.
(37) Gölander, C.-G.; Lin, Y-S.; Andrade, J. D. *Colloids Surf.* **1990**, *49*, 289.
(38) Hlady, V. *Appl. Spectrosc.* **1991**, *45*, 1991.
(39) Chaudhury, M. K.; Whitesides, G. M. *Science* **1992**, *256*, 1539.
(40) Pitt, W. G. *J. Colloid Interface Sci.* **1989**, *133*, 223.
(41) Lee, J. H.; Kim, H. G.; Khang, G. S.; Lee, H. B.; Jhon, M. S. *J. Colloid Interface Sci.* **1992**, *151*, 563.
(42) Lee, J. H.; Lee, H. B. *J. Biomater. Sci. Polym. Ed.* **1993**, *4*, 467.
(43) Lin, Y. S.; Hlady, V., Gölander, C.-G. *Colloids Surf. B: Biointerfaces* **1994**, *3*, 49.

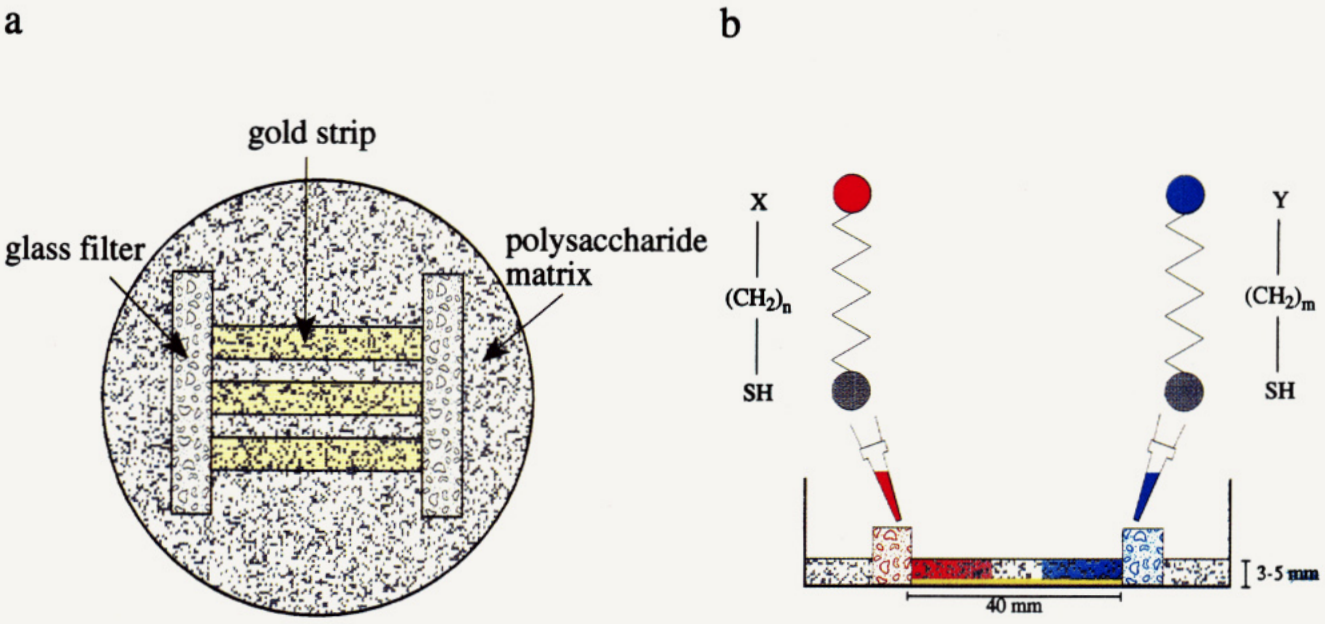


**Figure 1.** Schematic diagram of the (a) top and (b) side views of the cross-diffusion geometry used for the preparation of the molecular gradients. The polysaccharide matrix consists of Sephadex LH-20. The glass filters (100−150 μm pore size) are separated 40 mm and act as a supply for the thiol solutions.

measured directly on the screen of the video monitor and averaged to represent the correct contact angles within ±2°.

**Infrared Measurements.** The infrared reflection−absorption spectroscopy (IRAS) experiments were performed with a Bruker IFS 113v FT-IR spectrometer attached to an in-house customized ultrahigh vacuum system equipped with a manual sample scanning and manipulation system. The infrared beam was aligned at an 82° angle of incidence with respect to the surface normal and focused onto a ~1 mm spot on the sample surface using *f*/16 optics.[9] A narrow band MCT detector was used to detect the light, and 1000 consecutive scans were averaged at 4 $cm^{-1}$ resolution before Fourier transformation. All spectra are plotted as $-\log(R/R_0)$ where $R$ and $R_0$ are the reflectivities of the gold sample with and without the monolayer, respectively.

## Results and Discussion

**Preparation of Molecular Gradients.** Figure 1 shows the top and side views of the "cross-diffusion" setup used to prepare the molecular concentration gradients on gold. Gold strips cleaned in ethanol were placed on the bottom of a glass Petri dish (i.d. = 75 mm). The diffusion matrix was formed on top of the gold strips by mixing 6 g of Sephadex LH-20 and 18 g of ethanol (95%). Sephadex LH-20 is a chromatography material that can be handled in a broad range of organic solvents. It is normally used for separation of fatty acids, vitamins, hormones, and other relatively small organic molecules. Glass filters with a pore size of ~100−150 μm were gently pressed into the matrix 40 mm apart. The Sephadex was then allowed to homogenize during evaporation of excess ethanol until a ≈5 mm thick, completely swollen (3.3 mL EtOH/g Sephadex LH 20) diffusion matrix was formed on top of the gold strips. This diffusion geometry (length) was kept constant throughout this study, regardless of sample size and shape. The two thiol solutions, 200 μL (2 mM in EtOH), were then pipetted into the two glass filters and allowed to diffuse into the matrix with a diffusion front geometry determined by shape of the glass filters. We have not in detail investigated how the pore size of the glass filters influences the diffusion front geometry and thereby the quality of the gradients. However, a too small pore size, <2−5 μm, results in a nonuniform distribution of the thiol solution in the glass filters and consequently in an inhomogeneous diffusion front.

The entire setup was sealed in order to prevent additional evaporation of the solvent. The diffusion process was interrupted after 48 h. The gradients were then rinsed copiously in distilled water and ethanol and then ultrasonicated for 5 min in ethanol and water to ensure that all Sephadex LH 20 was completely removed from the surface. This cleaning procedure was normally found to be sufficient for gradients prepared from thiols with simple tail groups. It should be emphasized, however, that the interaction between the surface and the matrix may vary with the nature of the tail groups and that a unique cleaning protocol has to be developed for more complex combinations of thiols. It is also worth mentioning that it is possible to cross-diffuse another pair of components (thiols) in a direction perpendicular to the first pair.

**Ellipsometry and Contact Angle Measurements.** Figure 2 shows the ellipsometric thicknesses obtained for a series of molecular gradients prepared by cross-diffusion of ω-substituted alkanethiols with different tail groups and/or chain lengths. The ellipsometric thicknesses of two differently prepared $HS(CH_2)_{16}OH/HS(CH_2)_{15}CH_3$ ($OH/CH_3$) gradients are shown in Figure 2a. The top curve (unfilled circles) represent a gradient prepared during 48 h. The measured thicknesses are identical to those obtained in recent controlled composition, mixed monolayer studies[9,44] and varies continuously from 21.5 ± 1 Å on the far OH side to 19.5 ± 1 Å on the far $CH_3$ side. The cross-diffusion process itself limits drastically the number of molecules available for binding to the gold surface, as compared to a normal self-assembly process undertaken from 1−5 mM solutions (EtOH) of alkanethiols. The lower curve in Figure 2a (filled circles) illustrates what happens if the cross-diffusion experiment is interrupted too early, after ≈20 h. The reduced thicknesses in the gradient region (to about 50% of the thicknesses at the extreme ends) clearly suggest an incompletely covered gold surface consisting of a "precursor film" with conformationally disordered hydrocarbon chains. Thus, the diffusion time obviously is a critical preparation parameter which must be carefully considered. The effect becomes especially

(44) Parikh, A. N.; Liedberg, B.; Atre, S. V.; Ho, M.; Allara, D. L. *J. Phys. Chem.* **1995**, *99*, 9996.

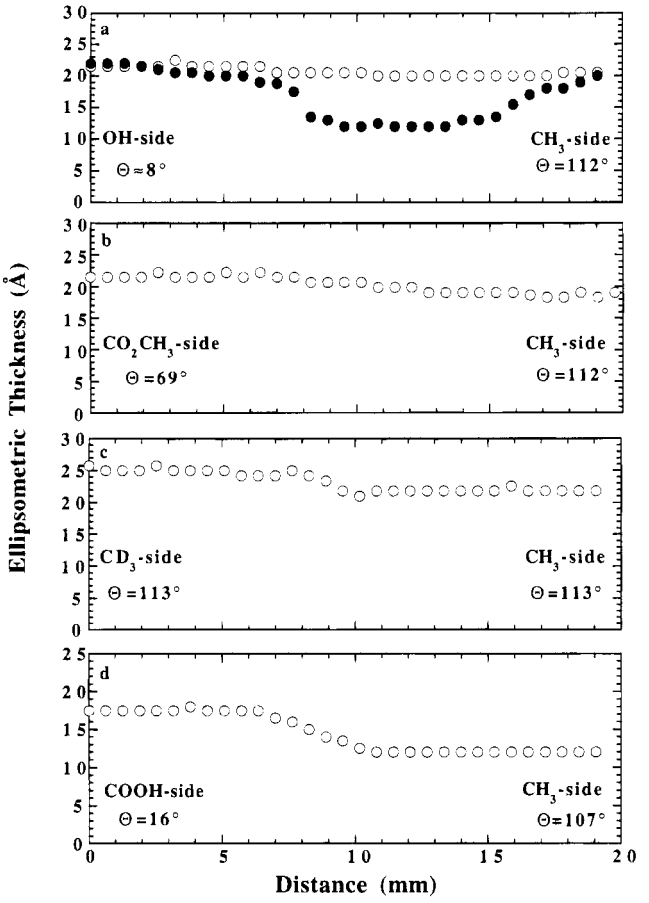


**Figure 2.** Ellipsometric thicknesses for a series of gradients: (a) $HS(CH_2)_{15}OH/HS(CH_2)_{15}CH_3$, where unfilled circles represent a gradient prepared for 48 h and filled circles a gradient prepared overnight, ≈20 h; (b) $HS(CH_2)_{15}CO_2CH_3/HS(CH_2)_{15}CH_3$; (c) $HS(CD_2)_{19}CD_3/HS(CH_2)_{17}CH_3$; (d) $HS(CD_2)_{10}COOH/HS(CH_2)_9CH_3$. The static contact angles with water Θ, determined at the very extreme ends of the gradient are also shown.

important in cases when high molecular weight ($M_w$) diffusion pairs are employed, a phenomenon related to the $M_w$ dependence of the diffusion constant $D \propto 1/\sqrt{M_w}$. We found, however, that a cross-diffusion time of 48 h was sufficient for the combinations of thiols used in this study.

A very similar behavior to that of the $OH/CH_3$ gradient is observed for the $HS(CH_2)_{15}CO_2CH_3/HS(CH_2)_{15}CH_3$ ($CO_2CH_3/CH_3$) gradient (Figure 2b) with a thickness of 21.5 ± 1 Å on the $CO_2CH_3$ side and 19.5 ± 1 Å on the $CH_3$ side. These thicknesses are also close to recently reported data[45] and to those expected from space-filling models if one assumes a polymethylene chain tilt of about 38° with respect to the surface normal.[4] Thus, it seems reasonable to assume that the gradient monolayers are composed of densely packed and highly oriented polymethylene chains. It is difficult to accurately identify the position of the gradient region for equally long thiols by using ellipsometry alone. However, the technique becomes readily useful when diffusion pairs of dissimilar chain lengths and/or tail groups are used (Figure 2c,d). For example, the increase in thickness of about 2.5–3 Å when moving from the $CH_x$ into the $CD_x$ side for the $HS(CD_2)_{19}CD_3/HS(CH_2)_{17}CH_3$ ($CD_3/CH_3$) gradient (Figure 2c) is in good agreement with the expected thickness difference of two methylene units.

The thickness of the $HS(CD_2)_{10}COOH/HS(CH_2)_9CH_3$ ($COOH/CH_3$) gradient is 17 ± 1 Å at the far COOH side

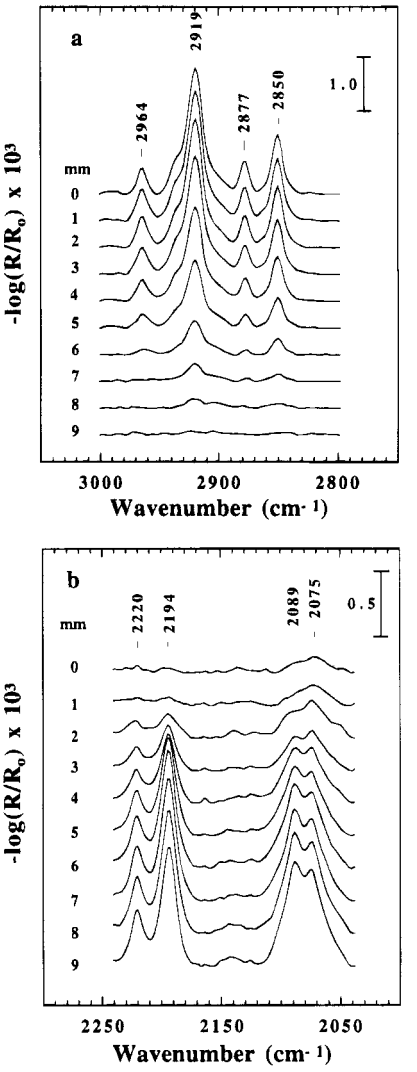


**Figure 3.** IRAS spectra of the (a) $CH_x$ and (b) $CD_x$ stretching regions of a $HS(CD_2)_{19}CD_3/HS(CH_2)_{17}CH_3$ gradient.

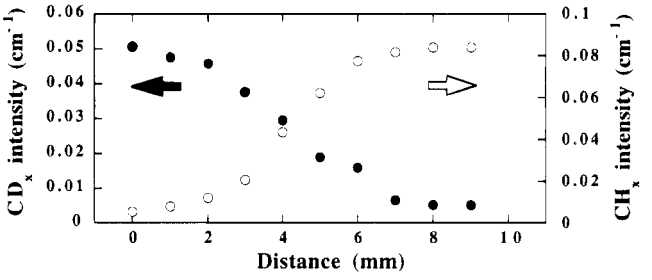


**Figure 4.** Integrated intensities of the $CD_x$ (2040–2240 $cm^{-1}$) and $CH_x$ (2820–2980 $cm^{-1}$) stretching regions of the ($CD_3/CH_3$) gradient (Figure 3).

(Figure 2d). This thickness agrees again well with previously reported values[3] and with thicknesses obtained from an ongoing study at our laboratory of single component monolayers of $HS(CD_2)_{10}COOH$ and $HS(CH_2)_{10}COOH$ on gold. The drop in thickness ≈5 Å when moving into the $CH_3$ side may look too large according to simple space-filling models. However, one of the early investigations[46] of the chain structure of $HS(CH_2)_nCH_3$ on gold with infrared spectroscopy, ellipsometry, and electrochemistry clearly pointed out that the *gauche* content rapidly increased for chain lengths $n < 10$. The monolayer

(45) Engquist, I., Lestelius, M.; Liedberg, B. Submitted to *J. Phys. Chem.*

(46) Porter, M. D.; Bright, T. B.; Allara, D. L.; Chidsey, C. E. D. *J. Am. Chem. Soc.* **1987**, *109*, 3559.

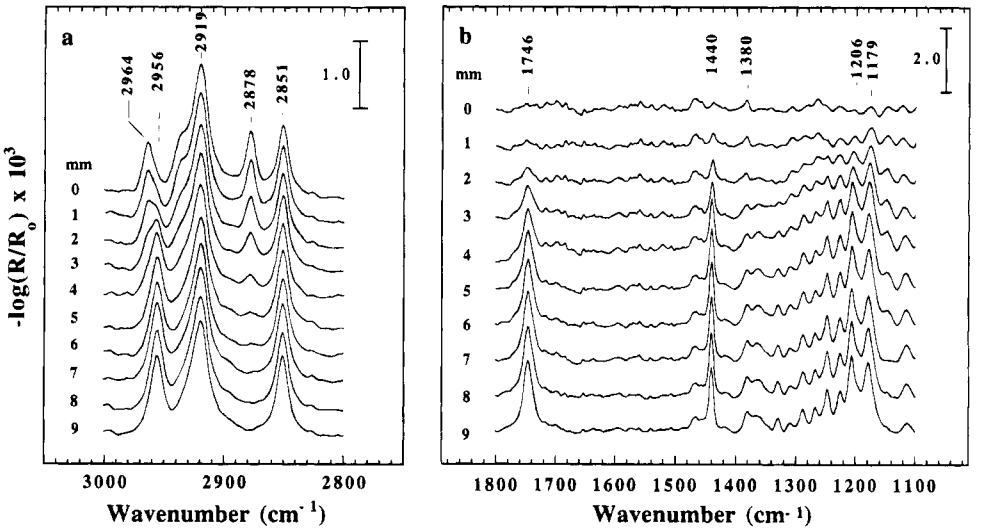


**Figure 5.** IRAS spectra of (a) the $CH_x$ stretching and (b) the tail group regions of a $HS(CH_2)_{15}CO_2CH_3/HS(CH_2)_{15}CH_3$ gradient.

thicknesses also started to deviate (decrease) from the expected thickness for a highly organized *all-trans* assembly. We believe that a partial disordering of the hydrocarbon chains on the $CH_3$ side of the gradient is responsible for the relatively large drop in thickness. It should be pointed out, however, that we are using the same refractive index, $n = 1.5$, for the COOH and the $CH_3$ side of the gradient. A refractive index of 1.45 is perhaps more representative for disordered (liquidlike) assembly, and an attempt to fit the ellipsometric data on the far $CH_3$ side with n = 1.45 results in an increase of the thickness with ≈1.5−2.0 Å. Thus, a more rigorous treatment of the ellisometric data suggests that the drop in thickness is slightly less than 5 Å, as shown in Figure 2d, perhaps only 3.0−3.5 Å. Most importantly, however, our results clearly indicate that the $CH_3$ side is more disordered than the COOH side. This conclusion is supported by the contact angle measurements (also depicted in Figure 2) which reveal that the $CH_3$ side, $\Theta = 107 \pm 2°$, has a large population of $-CH_2-$ groups exposed at the outermost surface.

Figure 2 shows the limiting contact angles with water at the very extreme ends of the gradients. The contact angles are also in good agreement with the values obtained for the corresponding single component monolayers. A thorough study of the wettability behavior of the gradients is under way and will be published separately. Nevertheless, our present set of ellipsometric and contact angle data clearly indicates that the gradient monolayers (at least for chain lengths >10) are composed of densely packed and highly oriented molecules, most likely with the polymethylene chains organized in a fully extended *all-trans* conformation. It is, however, not possible to accurately determine the exact position and the lateral dimension (length) of the gradient region from the ellipsometric data alone, unless the thiols exhibit very different tail groups and/or chain lengths. Spectroscopic techniques are therefore required to address this issue in more detail as will be shown below.

**Infrared Measurements.** In order to explore the chemical compositions, chain conformations, and lateral dimensions of the gradients in more detail we performed a series of scanning infrared reflection−absorption spectroscopy (IRAS) experiments. IRAS spectra of the ($CD_3$/$CH_3$) gradient are displayed in Figures 3a,b. The spectra show the $CH_x$ and $CD_x$ stretching regions as recorded with a step size of 1 mm over a total distance of 10 mm, the maximum scanning distance allowed with the sample

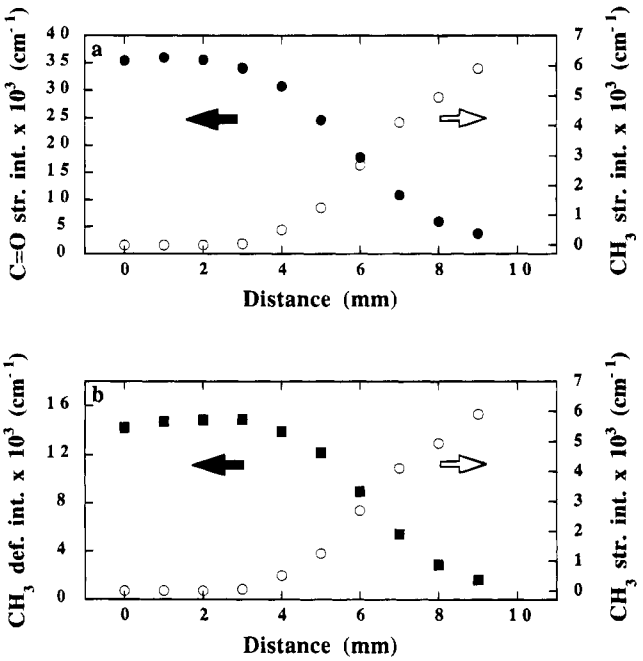


**Figure 6.** Integrated intensities of (a) the C=O mode at 1746 $cm^{-1}$ vs the symmetric $CH_3$ stretching mode of the *n*-alkanethiol at 2878 $cm^{-1}$; (b) the symmetric deformation mode of the methyl ester group at 1440 $cm^{-1}$ vs the $CH_3$ stretching mode of the *n*-alkanethiol at 2878 $cm^{-1}$. The center of the gradient is unfortunately offset about 1−2 mm with respect to the center of the gold substrate, making it impossible to scan all the way into the far $CH_3$ side.

holder design used in our ultrahigh vacuum system. The progression of the $CH_x$ and $CD_x$ stretching intensities and the absolute intensities at the extreme ends confirm the existence of two opposing concentration gradients. A detailed analysis of the infrared spectrum in the methylene stretching region can provide revealing information about the conformational status of the polymethylene chains. Snyder et al.[47−50] have extensively studied the infrared spectrum of polymethylenes in various physical states and

(47) Maroncelli, M.; Qi, S. P.; Strauss, H. L.; Snyder, R. G. *J. Am. Chem. Soc.* **1982**, *104*, 6237.
(48) MacPhail, R. A.; Strauss, H. L.;Snyder, R. G.; Elliger, C. A. *J. Phys. Chem.* **1984**, *88*, 334.
(49) Snyder, R. G.; Strauss, H. L., Elliger, C. A. *J. Chem. Phys.* **1982**, *86*, 5145.
(50) Snyder, R. G.; Maroncelli, M.; Strauss, H. L.; Hallmark, V. M. *J. Chem. Phys.* **1986**, *90*, 5623.

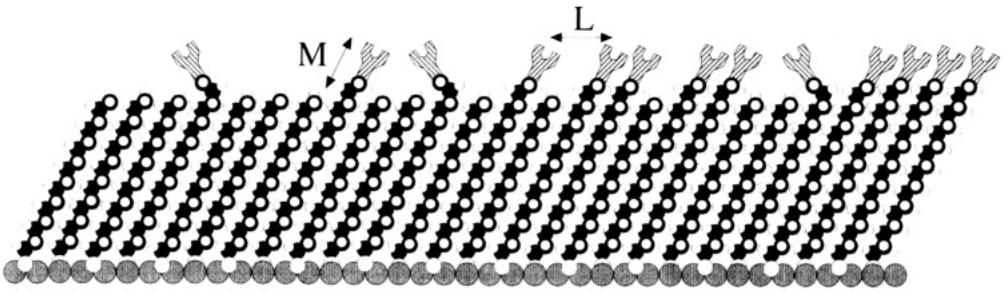


**Figure 7.** Schematic diagram showing a gradient of molecular interaction sites (e.g. receptor−ligand). Two important parameters are identified: $L$ is the average distance between sites, and $M$ the mobility of the protruding methylene tails (see the text for discussion).

they found that crystalline *all-trans*-polymethylenes exhibited $CH_2$ symmetric ($d^+$) and antisymmetric ($d^-$) stretching modes close to 2850 and 2916 $cm^{-1}$, respectively, whereas the same peaks for liquidlike gauche-rich polymethylenes increased to 2856 and 2928 $cm^{-1}$, respectively. Recently reported IRAS spectra of the very best single component alkanethiol monolayers on the coinage metals,[5] prepared from thiols of similar chain length as those used here, exhibit $d^+$ and $d^-$ peaks near 2850 and 2918 $cm^{-1}$, respectively. These frequencies are normally considered as strong evidence for the formation of highly organized assemblies with low *gauche* defect density, i.e., *all-trans*-polymethylenes. The *n*-alkanethiols also exhibit characteristic $CH_3$ symmetric ($r^+$) and asymmetric ($r^-_a$) stretching modes at 2879 and 2964 $cm^{-1}$,[5,46] respectively. The corresponding modes appear at 2877 and 2964 $cm^{-1}$ in the gradient spectra (Figure 3a). The $CD_x$ modes of fully deuterated polymethylenes have not been as thoroughly characterized as the $CH_x$ modes. The $CD_x$ modes at 2220, 2194, 2089, and 2075 $cm^{-1}$ for the gradient samples appear, however, very close to those observed for a single component monolayer of $HS(CD_2)_{19}CD_3$ (2219, 2193, 2089, and 2074 $cm^{-1}$), indicating a very similar chain structure. The peak intensities of the $CH_x$ and $CD_x$ modes are also in agreement with the observed intensities for the single component monolayers. Thus, the most plausible conclusion from the IR measurements is that the gradient assembly predominantly consists of conformationally ordered *all-trans* chains. The small upward shift ~1 $cm^{-1}$ of the $d^-$ mode in the gradient spectra (the most sensitive indicator for disordered components within the polymethylene chains) suggests a slightly increased fraction of *gauche* conformers as compared to single component assemblies. The *gauche* conformers are most likely located at the outermost portion of the chains.

The lateral dimension of the $CH_3/CD_3$ gradient has been determined from the intensities of the $CH_x$ and $CD_x$ modes, respectively. Figure 4 shows a plot of the integrated intensities of the $CH_x$ (2820−2980 $cm^{-1}$) and $CD_x$ (2040−2240 $cm^{-1}$) for the gradient spectra in Figure 3. From these data we conclude that the cross-diffusion methodology illustrated in Figure 1 can be used to generate smooth and continuous concentration gradients on gold. For this particular combination of $\omega$-substituted *n*-alkanethiols the length of the gradient turned out to be approximately 6−8 mm. It is worth mentioning that the present IR scanning methodology most likely overestimates the length of the gradient region because of the relatively large spot size of the IR beam (≈1 mm). Preliminary small spot (≈200 $\mu$m) X-ray photoelectron spectroscopy (XPS) data for a series of analogous gradients suggests that the lower value is more representative of the *true* gradient length. Shorter gradients can be prepared by reducing the distance between the glass filters (Figure 1) or by using short chain thiols with higher diffusion constants. The $HS(CD_2)_{10}COOH/HS(CH_2)_9CH_3$) gradient, for example, is, according to the ellipsometric data in Figure 2d, about 4−5 mm long.

Gradients with dissimilar tail groups have also been analyzed with IRAS, and Figure 5 shows spectra from both the $CH_x$ and the tail group regions of a ($CO_2CH_3/CH_3$) gradient (*cf.* Figure 2b). The methyl ester thiol exhibits three characteristic modes in the $CH_x$ stretching region at 2851, 2919, and 2956 $cm^{-1}$, respectively. The frequencies of the $CH_x$ modes of the methyl ester thiol and those of the *n*-alkanethiol agree very well with reported values for single component monolayers.[4,45] The tail group region (Figure 5) displays a number of peaks characteristic for the methyl ester thiol including the carbonyl ester C=O mode at 1746 $cm^{-1}$, the symmetric $CH_3O$ (CH3) bending mode at 1440 $cm^{-1}$, and two C-O stretching modes at 1206 and 1179 $cm^{-1}$, respectively. A series of well-resolved peaks due to chain wagging and twisting motions, the so-called progression bands,[47] also can be found in the 1350−1200 $cm^{-1}$ region. The appearance of these latter modes and the low $d^-$ frequency at 2919 $cm^{-1}$ throughout the gradient region clearly support the general picture of a highly organized *all-trans* gradient assembly.

Moreover, we have used the integrated intensities of the C=O stretching mode at 1746 $cm^{-1}$, the $CH_3$ deformation mode at 1440 $cm^{-1}$ of the methyl ester group, and the $CH_3$ stretching mode at 2878 $cm^{-1}$ of the *n*-alkanethiol to estimate the length of the gradient (Figure 6). Although we were unable to collect spectra at the far $CH_3$ side, the gradient region appears to be about 6−8 mm long in this case as well, (*cf.* Figure 4).

The present cross-diffusion methodology undoubtedly allows us to generate molecular concentration gradients of $\omega$-substituted alkanethiols on gold. The ellipsometric and infrared data clearly indicate that the gradient assemblies are structurally very similar to the corresponding single component and mixed composition SAMs. The experimental geometry and the present model system enable us to prepare gradients extending over macroscopic distances, several millimeters. However, we are yet not able to present conclusive evidence for a smooth variation in chemical composition on all levels of molecular complexity, i.e., all the way down to the molecular (nm) scale. Scanning tunnelling microscopy (STM) or scanning force microscopy (SFM) are techniques that must be employed to investigate whether the mixing of the two thiols occurs homogeneously in the gradient region or in the form of patches/islands. Nor can we from the present set of data exclude the possibility that so-called "fingering" phenomena occurs when the two diffusion fronts meet. Fingering will inevitably result in an inhomogeneous diffusion front and in a varying chemical composition in the direction perpendicular to the gradient. Small spot XPS and secondary ion mass spectroscopy (SIMS) are currently employed to address this issue.

The present gradient method can certainly be used to address a broad range of new and interesting applications of alkanethiolate self-assembled monolayers (SAMs), many of which are impossible to foresee today. The work of Elwing and co-workers[29-35] clearly demonstrated the advantage of using a single gradient surface rather than a large number of fixed composition surfaces for studies of wettability-induced protein interaction phenomena on solid surfaces. The numerous chemical and structural combinations accessible with the present approach opens the possibility to generate unique architectures that hardly can be obtained with the chlorosilane/$SiO_2$ chemistry nor with the Langmuir–Blodgett technique. The robustness of the alkanethiolate/Au system offers also the possibility to employ standard organic synthetic chemistry to further modify the chemical properties of the substrate surface. Thus, the gradients can act as a well-defined template for the immobilization of complex biomolecules and for controlled distribution of molecular recognition centers.

A common feature of many recognition processes, like receptor–ligand interactions, is that they are site-specific, meaning that the sterical requirements for the interaction may be governed by the local chemical environment. For example, a receptor may only be active if it is embedded in an unique chemical pocket. Cooperative interactions between receptor sites may also be of importance for the outcome of the interaction, i.e., the average distance between receptor sites, $L$, as well as their mobility (accessibility), $M$, may influence the receptor–ligand interaction (Figure 7). We believe that molecular gradients can be an excellent tool to mimic and to learn more about the sterical requirements for such reactions. The most obvious application of the gradients is perhaps to use them as a first "screening tool" to identify whether or not there exist a critical or optimal surface parameter for the interaction with the ligand.

There exists today a large number of imaging methods with sufficient lateral resolution and sensitivity (SIMS, XPS, fluorescence, STM, and SFM) which, depending of the size and complexity of the molecular system, can help us identify where along the gradient surface the interaction has occurred or, alternatively, not occurred. This particular position on the surface can then be identified to represent a certain composition (density of interaction sites) or, alternatively, even more complex physical parameters like net charge, $pK_a$, surface energy, L- or D-isomerism.

Affinity biosensors also rely on molecular recognition processes, and much of the above discussion about receptor–ligand interaction is directly applicable to the design and development of biosensing interfaces.

## Conclusions

This paper describes a cross-diffusion methodology capable of generating a molecular concentration gradient on a solid support. We have chosen a model system consisting of long chain ω-substituted $n$-alkanethiols thiols and polycrystalline gold. This system was selected because of its robustness and ease of handling. Thiols on gold are generally also considered to be the most flexible synthetic methodology for the generation of well-defined organic surface phases, SAMs, with molecular level control over composition and chain conformation. The structure, composition, and lateral dimensions of a series of gradients have been exploited by using single wavelength ellipsometry, contact angle measurements, and infrared spectroscopy. The ellipsometric and infrared data inevitably support the formation of highly organized and densely packed *all-trans* gradient assemblies (for thiols with a chain length >10) that extend over macroscopic distances ≈4–8 mm.

We find these gradients very attractive as model organic substrates for detailed studies of a broad range of interfacial phenomena. More detailed investigations describing their microscopic structure and mixing behavior, as well as some of their potential applications, are under way. The mixing behavior in the gradient region is especially important for the application of these novel gradients in areas related to molecular recognition and biosensing.

**Acknowledgment.** This research was supported by grants from the Swedish Research Council for Engineering Sciences (TFR), the Swedish National Board for Technical and Industrial Development (NUTEK) and the Swedish Natural Science Research Council (NFR) through the Swedish Biomaterials Consortium.

LA9502608